DALTON

Racemization kinetics and spin states of four-co-ordinate nickel(II) N_2X_2 Schiff-base and aza complexes with bi- or tetra-dentate ligands incorporating pyrazole (X = NH or S)†

Agnete la Cour,*[a] Matthias Findeisen,[b] Kim Hansen,[c] Rita Hazell,[c] Lothar Hennig,[d] Carl E. Olsen,[e] Lars Pedersen[c] and Ole Simonsen[a]

[a] *Department of Chemistry, Odense University, DK-5230, Odense M, Denmark*
[b] *Department of Analytical Chemistry, Leipzig University, D-04103 Leipzig, Germany*
[c] *Department of Chemistry, Aarhus University, DK-8000 Århus C, Denmark*
[d] *Department of Organic Chemistry, Leipzig University, D-04103 Leipzig, Germany*
[e] *Department of Chemistry, The Royal Veterinary and Agricultural University, DK-1871 Frederiksberg C, Denmark*

Bis(bidentate ligand) and tetradentate ligand nickel(II) N_2X_2 Schiff-base and aza complexes (X = NH or S) have been prepared and their properties investigated by spectroscopic methods. In the bis(bidentate ligand) complexes the aza function stabilizes the low-spin $S = 0$ state compared with the imine function. The aza complexes are low spin both in the solid state and in solution; the Schiff-base complexes are either low or high spin ($S = 1$) in the solid state, and are either in spin equilibrium ($S = 0 \rightleftharpoons S = 1$) or high spin in solution. The crystal structure has been solved for the high-spin complex bis(4-isopropyliminomethyl-1,3-diphenylpyrazol-5-ylaminato)nickel(II). The co-ordination of Ni is pseudo-tetrahedral, the angle between the N–Ni–NH and NH′–Ni–N′ planes being 93.8(1)°. The Ni–N (imine) bond lengths are 1.999(2) and 2.003(3) Å, significantly longer than the Ni–N (amine) bond lengths of 1.919(2) Å. In the tetradentate ligand complexes the two identical halves of the ligands are linked by aliphatic four-carbon chains. When the linkage is $CMe_2(CH_2)_2CMe_2$ the complexes are fully paramagnetic in the solid state and in solution, while complexes bridged by unsubstituted $(CH_2)_4$ are low spin in the solid state and in spin equilibrium in solution. The crystal structure of [*N*,*N*′-bis(1,3-dimethyl-5-sulfanylpyrazol-4-ylmethylene)butane-1,4-diaminato]nickel(II) reveals an almost planar co-ordination geometry, the angle between the N–Ni–S and S′–Ni–N′ planes being 7.9(3)°. The Schiff-base complexes are chiral and all show evidence of racemization in solution. Thermodynamic parameters for the spin-equilibrium process in CD_2Cl_2 [ΔG(25 °C) from −4.32 to 0.71 kJ mol^{-1} for the bis(bidentate ligand) systems, from 3.72 to 11.3 kJ mol^{-1} for the tetradentate ligand systems] and kinetic parameters for the racemization process in CD_2Cl_2 or $CDCl_2CDCl_2$ [$\Delta G^{\ddagger}$(25 °C) from 40.5 to 53.3 kJ mol^{-1} for the bis(bidentate ligand) complexes, 46.5 to 63.1 kJ mol^{-1} for the tetradentate ligand complexes] have been derived using variable-temperature ^{1}H NMR spectroscopy. Sulfur donor atoms and aryl substituents favour the low-spin state. Ligand-field parameters for the Schiff-base complexes have been derived from the electronic spectra.

It is well known that pseudo-tetrahedral complexes of nickel(II) will often be involved in the spin-equilibrium process (1)[1] where

$$S = 0 \rightleftharpoons S = 1 \quad (1)$$

S is the total electronic spin and in the racemization process (2)[2]

$$\Delta \rightleftharpoons \Lambda \quad (2)$$

where Δ (D) and Λ (L) refer to the absolute configuration of the co-ordination sphere. Rate constants for the racemization process are often of the order of ms^{-1} at room temperature, that is within the NMR timescale, and the resonances derived from diastereotopic protons of racemizing systems can often be frozen out in ^{1}H NMR spectra.[2] The spin-equilibrium process is in general very much faster with rate constants of the order of ps^{-1} and a freezing out of the low- and high-spin forms in ^{1}H NMR spectroscopy has been reported only for dihalogenobis(phosphine)nickel(II) complexes.[1a,b]

In previous work[2c] one of us investigated possible relations between the spin-equilibrium process (1) and the racemization process (2) in a series of pseudo-tetrahedral bis(bidentate ligand)nickel(II) Schiff-base complexes with N_2S_2 co-ordination spheres. For three systems having mole fractions of high-spin molecules close to unity the racemization process most probably followed a pseudo-rotation route in which a planar and possibly low-spin form of the complex is an intermediate. A correlation might therefore be expected between the rate of the racemization and a large mole fraction of planar low-spin molecules. The previous study of three complexes with similar magnetic properties did not permit a conclusion with respect to a correlation of that kind.

In order to continue these investigations of the racemization process for pseudo-tetrahedral Ni^{II} we have prepared chiral complexes with more distinct magnetic properties. Bis(bidentate ligand) complexes (type A) and tetradentate ligand complexes (type B) were prepared. In this paper tetradentate ligand complexes are marked with an asterisk, and **1***–**6*** linked by tetramethylene are pyrazolyl substituted in the same manner as the bis(bidentate ligand) complexes **1**–**6** with Pr^i substituents on the imine nitrogen-donor atoms.

† *Supplementary data available* (No. SUP 57244, 13 pp.): NMR data, equilibrium and rate constants, Eyring plots. See Instructions for Authors, *J. Chem. Soc., Dalton Trans.*, 1997, Issue 1.
Non-SI units employed: $\mu_B \approx 9.27 \times 10^{-24}$ J T^{-1}, D ≈ 3.33 × 10^{-30} C m.

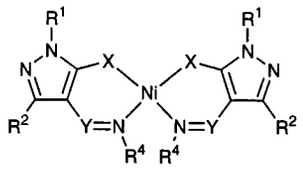

A

	X	Y	R^1	R^2	R^3	R^4
1	NH	CR^3	Ph	Ph	H	Pr^i
2[a]	S	CR^3	Ph	Ph	H	Pr^i
3[a]	S	CR^3	Me	Me	H	Pr^i
4[a]	S	CR^3	Ph	Me	H	Pr^i
5[a]	S	CR^3	Me	Ph	H	Pr^i
6[a]	S	CR^3	Me	*p*-ClC_6H_4	H	Pr^i
7	S	CR^3	Me	Ph	H	2, 6-$Me_2C_6H_3$
8	S	CR^3	Ph	Me	Ph	Ph
9	S	CR^3	Ph	Me	Ph	*p*-$H_2NC_6H_4$
10[b]	S	N	Ph	Me	-	Ph
11	S	N	Ph	Me	-	*p*-$Et_2NC_6H_4$

[a] First presented in ref. 2(*c*). [b] First presented in ref. 3

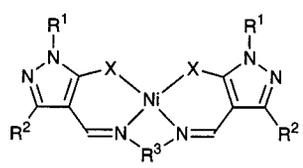

B

	X	R^1	R^2	R^3
1*[a]	NH	Ph	Ph	$(CH_2)_4$
$\mathbf{1}_{Me}$*	NH	Me	Ph	$(CH_2)_4$
2*	S	Ph	Ph	$(CH_2)_4$
3*	S	Me	Me	$(CH_2)_4$
4*	S	Ph	Me	$(CH_2)_4$
5*[b]	S	Me	Ph	$(CH_2)_4$
6*	S	Me	*p*-ClC_6H_4	$(CH_2)_4$
7*	S	Me	Me	$CMe_2(CH_2)_2CMe_2$
8*	S	Ph	Me	$CMe_2(CH_2)_2CMe_2$

[a] First presented in ref. 4(*a*). [b] First presented in ref. 4(*b*)

Results and Discussion

Syntheses and identification

Yields and some analytical data are presented in Table 1. Crystals of the complexes tend to incorporate the solvent used for recrystallization, as is also observed for other $M^{II}N_2X_2$ complexes containing 1,3-disubstituted pyrazolyl [see *e.g.* refs. 4(*a*), (*c*)–(*e*)]. Even after drying the complexes under vacuum at room temperature the elemental analyses show small amounts of occluded solvent (see Experimental section and Table 1). The tetradentate ligand $N_2(NH)_2$ complexes **1*** and $\mathbf{1}_{Me}$* seem to take up small amounts of water. Analyses of these complexes dried at room temperature are best fitted if one (for **1***) or one half (for $\mathbf{1}_{Me}$*) molecule of water is included per complex. However, when **1*** is dried over P_2O_5 at 50 °C for 12 h immediately before elemental analyses the water and most crystal solvent are lost (see Table 1). Impurities were not observed in the ^{1}H NMR spectra of the complexes.

Crystal structures

Complex 1. Selected bond lengths and angles are listed in Table 2(*a*); the molecular structure is shown in Fig. 1. The complex has approximately two-fold symmetry. The co-ordination geometry is pseudo-tetrahedral, the angle θ between the N(1)–Ni–N(8) and N(18)–Ni–N(11) planes being 93.8(1)°.‡ The Ni–N bond lengths are similar to those of other paramagnetic $N_2(NR)_2$ complexes with conjugated six-membered chelate rings[5a,b] [see Table 2(*b*), complexes **a** and **b**] and longer than those in diamagnetic complexes with similar ligands[4a,5c–f] [see Table 2(*b*), complexes **1***, **c**, **d*** and **e***].

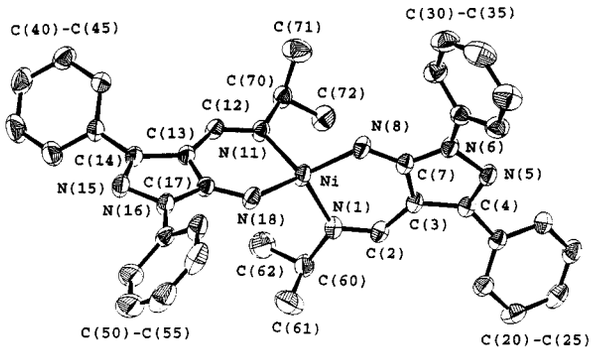

Fig. 1 Molecular structure of complex **1** with 50% probability thermal ellipsoids

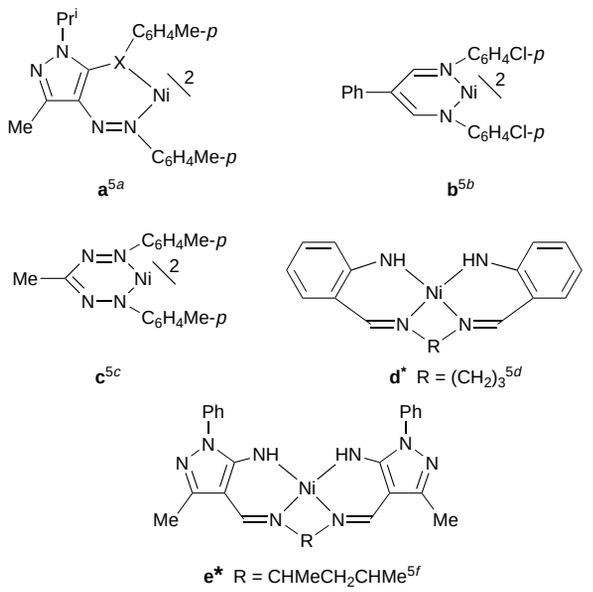

Complex 3*. Selected bond distances and angles are listed in Table 3(*a*); the molecular structure is shown in Fig. 2. The structures of $M^{II}N_2S_2$ Schiff-base complexes with conjugated six-membered chelate rings have been reviewed recently.[6a] Structural information on nickel(II) complexes incorporating pyrazole, most of more recent date, are listed in Table 3(*b*) (structures **j***, **k**, see Table 3 footnote). The primary co-ordination sphere in complex **3*** is a flattened tetrahedron. The angle θ between the planes N(1)–Ni–S(8) and S(18)–Ni–N(11) is 7.9(3)°, which is smaller than the corresponding angle in complex **5***[4b] and in the similar $n = 4$§ complex **h***[6b] [Table 3(*b*)]. This flattening in **3*** may be due to the lower steric bulk of the pyrazolyl methyl substituents. Once again the co-ordination sphere in complexes bridged by polymethylene tends to be remarkably distorted from a two-fold symmetry.

‡ A N_2X_2 metal complex is defined *cis* if the angle θ between the normals to the planes N–M–X and X′–M–N′ is <90°, *trans* if this angle is >90°, M being the origin of a Cartesian coordinate system and N, X, X′ and N′ vectors in this system.

§ *n* is the length (number of carbon atoms) of the linkage bridging the two identical parts of a tetradentate ligand.

Table 1 Yields and analytical data for the complexes[a]

Complex	Crystal solvent	Yield[b] (%)	Analysis (%)[c] C	H	N	EI mass spectrum, *m*/*z*[d]
1[e]	0.10 $CHCl_3$	58	67.4 (67.55)	5.75 (5.65)	16.4 (16.55)	664
7[f]	$CHCl_3$	93	57.0 (57.2)	4.5 (4.55)	10.25 (10.25)	698
8		98	68.75 (69.45)	4.6 (4.55)	10.5 (10.55)	796[g]
9		96	66.05 (66.9)	4.6 (4.65)	13.45 (13.55)	824
10		90	59.35 (59.55)	4.05 (4.05)	17.35 (17.35)	644
11		91	59.55 (61.0)	5.5 (5.65)	17.15 (17.8)	786
1*[f]	1.50 $CHCl_3 \cdot H_2O$	92	54.35 (54.1)	4.2 (4.3)	13.35 (13.45)	634
1*[f,h]	0.15 $CHCl_3$		66.45 (66.45)	5.05 (4.95)	17.15 (17.15)	
$\mathbf{1}^*_{Me}$[f]	0.50 H_2O	19	60.15 (60.0)	5.6 (5.6)	21.1 (21.55)	510
2*[f]	0.85 $CHCl_3$	56	56.95 (57.55)	4.1 (4.05)	11.05 (10.95)	668
3*		98	46.0 (45.65)	5.4 (5.25)	19.0 (19.95)	420
4*[i]	0.35 CH_2CH_2	47	55.5 (54.95)	5.0 (4.7)	13.9 (14.6)	544
6*[f]	0.40 $CHCl_3$	90	47.45 (47.9)	3.8 (3.7)	13.0 (12.7)	614[g]
7*		59	49.9 (50.35)	6.2 (6.35)	17.15 (17.6)	476
8*		40	59.8 (59.9)	5.7 (5.7)	13.95 (13.95)	600

Complexes **8**–**11**, **3***, **7*** and **8*** were not recrystallized. [a] Complexes **2**–**6**, presented in ref. 2(*c*), and **5***, presented in ref. 4(*b*), together with their spectroscopic properties (NMR, UV/VIS/NIR) were prepared as described in these papers and identified from these spectroscopic properties. All complexes were dried as described in the Experimental section. [b] From ligand (when X = NH, from *o*-aminopyrazolecarbaldehyde). [c] Calculated values in parentheses. [d] Crystal solvent is not included in the molecular ion, M^+. [e] Recrystallized from MeOH–$CHCl_3$. [f] Recrystallized from $CHCl_3$. [g] $M^+ + 2$. [h] Dried at 50 °C for 12 h over *o*-aminopyrazolecarbaldehyde. [i] Recrystallized from CH_2Cl_2.

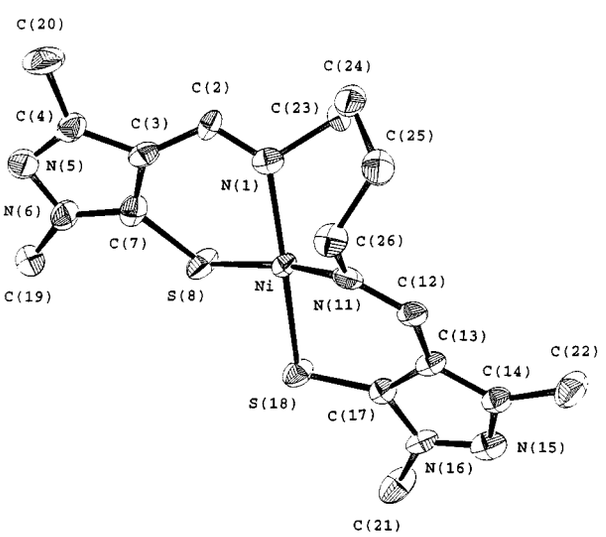

Fig. 2 Molecular structure of complex **3*** with 50% probability thermal ellipsoids

Magnetic properties

Room-temperature magnetic moments for the bis(bidentate ligand) complexes are in Table 4(*a*). Owing to the efflorescence of the crystal solvent in **1** and **7** (see Table 1) it has not been included in the calculations of the moments for these complexes. Complexes **1**–**6** are paramagnetic¶ and **7**–**11** are almost diamagnetic in the solid state. The small moments of about 1 μ_B for the latter are expected for low-spin nickel(II) complexes and are ascribed mainly to the temperature-independent paramagnetism of the nickel(II) ion.[1c] The Schiff-base complexes **1**–**9** are paramagnetic in solution. However, the rise in moment with temperature for **7**–**9** compared with that of a fully paramagnetic standard, $[Cr^{III}(acac)_3]$ (acac = acetylacetonate), indicates that these complexes are in spin equilibrium in solution in accord with the temperature-dependent ^{1}H NMR spectra (see below).

Plots of the chemical shifts *vs.* 1/*T* for complexes **1** and **3**–**6** yield straight lines for all protons except for the ones exchanging in the racemization process. This Curie-law dependence indicates that the mole fraction of high-spin molecules, N_{hs}, is equal to or very close to one in these complexes [see Experimental section, equation (4)[9]] in the investigated temperature range, from −100 (−65 for **3**) to 90 °C [low-temperature spectral data for complexes **4**–**6** were presented in ref. 2(*c*)]. The plots for **1** are shown in Fig. 3(*a*). A non-Curie-law dependence indicative of a spin-equilibrium process ($0 < N_{hs} < 1$) in which N_{hs} grows with temperature is observed for complexes **2** and **7**–**9**, see Fig. 3(*b*) for **8**.

The aza complexes **10** and **11** are low spin both in the solid state and in solution. The ^{1}H NMR spectra (Fig. 4) are typical of diamagnetic compounds. The aza function stabilizes the low-spin state compared with the imine function. This is also seen in $N_2(NR)_2$ complexes incorporating pyrazole. In a series of Ni^{II}-$N_2(NR)_2$ complexes with bidentate aza ligands (R = aryl or H) the complex that is most comparable with the Schiff-base complex **1** (R = H) is diamagnetic.[5a]

Room-temperature magnetic moments for the tetradentate ligand complexes are listed in Table 4(*b*). Owing to the efflor-

¶ A low magnetic moment (1.77 μ_B in the solid state at room temperature) is reported for a pyrazole-based bis(bidentate ligand) complex similar to **1** ($R^1 = R^4$ = Ph, R^2 = Me, R^3 = H).[8]

Table 2 Selected bond distances (Å) and angles (°) for complex **1** (*a*)[a] and comparison of bond lengths in the six-membered chelate rings for some $Ni^{II}N_2(NR)_2$ complexes with symmetrical conjugated ligands (*b*)[b]

(*a*)

Ni–N(1)	1.999(2)	N(8)–Ni–N(18)	123.3(1)	N(11)–C(12)–C(13)	124.9(2)
Ni–N(8)	1.919(2)	N(1)–Ni–N(8)	94.46(9)	C(12)–C(13)–C(17)	125.0(2)
Ni–N(11)	2.003(2)	N(8)–Ni–N(11)	115.72(9)	C(13)–C(17)–N(18)	126.4(2)
Ni–N(18)	1.919(2)	N(1)–Ni–N(18)	114.4(1)	Ni–N(18)–C(17)	124.5(2)
N(1)–C(2)	1.309(3)	N(11)–Ni–N(18)	94.23(9)		
C(2)–C(3)	1.405(4)	N(1)–Ni–N(11)	116.56(9)		
C(3)–C(7)	1.409(3)	Ni–N(1)–C(2)	124.3(2)		
C(7)–N(8)	1.329(3)	N(1)–C(2)–C(3)	125.1(2)		
N(11)–C(12)	1.302(3)	C(2)–C(3)–C(7)	125.0(2)	N(1)–Ni–N(8)/	93.8(1)[c]
C(12)–C(13)	1.407(4)	C(3)–C(7)–N(8)	126.4(2)	N(18)–Ni–N(11)	
C(13)–C(17)	1.411(3)	Ni–N(8)–C(7)	124.5(2)		
C(17)–N(18)	1.326(3)	Ni–N(11)–C(12)	124.4(2)		

(*b*)

Compound	Ni–N(1)	Ni–N(8)	N(1)–A(2)	A(2)–C(3)	C(3)–C(7)	C(7)–N(8)	Ref.
1	2.001	1.919	1.306	1.406	1.410	1.328	This work
a	1.952	1.931	1.295	1.325	1.420	1.335	5(*a*)
b	1.947	1.943	1.341	1.390	1.395	1.331	5(*b*)
c	1.869	1.861	1.318	1.341	1.330	1.313	5(*c*)
d*	1.923	1.860	1.34	1.38	1.40	1.36	5(*e*)
1*	1.913	1.873	1.304	1.399	1.409	1.319	4(*a*)
e1*	1.890	1.855	1.290	1.360	1.425	1.305	5(*f*)
e2*	1.885	1.855	1.300	1.395	1.360	1.340	

[a] Estimated standard deviations (e.s.d.s) of the least significant digits are given in parentheses. [b] The numbering is as for complex **1**; average distances for the two chelate rings are given; the asymmetric unit for **e*** contains two molecules, **e1*** and **e2***. The θ angles are 90.0, 21.5, 0, 2.3, 21, 16 and 14° for **a**, **b**, **c**, **d***, **1***, **e1*** and **e2***, respectively; atom A is carbon (**1**, **b**, **d***, **1*** and **e***) or nitrogen (**a** and **c**). [c] Angle θ.

Table 3 Selected bond distances (Å) and angles (°) for complex **3*** (*a*)[a] and for $Ni^{II}N_2S_2$ Schiff-base complexes incorporating pyrazole (*b*)[b]

(*a*)

Ni–N(1)	2.001(8)	S(8)–Ni–S(18)	81.1(1)	N(11)–C(12)–C(13)	119(1)
Ni–S(8)	2.195(4)	N(1)–Ni–S(8)	92.9(3)	C(12)–C(13)–C(17)	125(1)
Ni–N(11)	1.867(9)	S(8)–Ni–N(11)	171.4(3)	C(13)–C(17)–S(18)	131.2(9)
Ni–S(18)	2.188(4)	N(1)–Ni–S(18)	172.7(3)	Ni–S(18)–C(17)	103.6(4)
N(1)–C(2)	1.26(1)	N(11)–Ni–S(18)	94.4(3)		
C(2)–C(3)	1.39(2)	N(1)–Ni–N(11)	92.1(4)		
C(3)–C(7)	1.43(2)	Ni–N(1)–C(2)	130.1(8)		
C(7)–S(8)	1.77(1)	N(1)–C(2)–C(3)	122(1)	N(1)–Ni–S(8)/	7.9(3)[c]
N(11)–C(12)	1.37(1)	C(2)–C(3)–C(7)	128(1)	S(18)–Ni–N(11)	
C(12)–C(13)	1.43(2)	C(3)–C(7)–S(8)	124.3(9)		
C(13)–C(17)	1.39(1)	Ni–S(8)–C(7)	103.4(4)		
C(17)–S(18)	1.67(1)	Ni–N(11)–C(12)	131.8(8)		
S(8)···S(18)	2.850(5)				

(*b*)

Compound	*n*	Ni–N	Ni–S	N=C	S–C	S···S′	S–Ni–S′	θ	Ref.
f*	2	1.902	2.185	1.287	1.708			5.7	4(*a*)
		1.916	2.183	1.281	1.706				
g_1*	3	1.88	2.18	1.26	1.65	2.88	81.3	7.2	6(*a*)
		1.89	2.24	1.29	1.65				
g_2*	3	1.97	2.21	1.31	1.77	2.88	81.4	10.2	
		1.91	2.21	1.29	1.71				
h*	4	1.943	2.173	1.295	1.718			18.3	4(*a*)
		1.917	2.211	1.293	1.716				
5*	4	1.932	2.196	1.298	1.725	2.858	81.4	12.7	1(*c*)
		1.935	2.187	1.295	1.723				
i*	4	1.966	2.240			3.834	117.6	77.4	4(*b*)
		1.965	2.244						
j*	4	1.927	2.185			2.850	81.4	35.7	4(*b*)
k	—	1.989	2.249	1.287	1.717	3.639	108.0	82.4	1(*a*)

[a] Estimated standard deviations (e.s.d.s) of the least significant digits are given in parentheses. [b] For each complex the pyrazolyl substituents are given in the order R^1, R^2, R^3 (see type A and B complexes above): **f*** Pr^i, Me, $(CH_2)_2$; **g*** Ph, Me, $(CH_2)_3$ (two molecules in the asymmetric unit); **h*** Pr^i, Me, $(CH_2)_4$; **i*** Me, Me, 6,6′-dimethyl-2,2′-biphenyl; **j*** Ph, Me, 2,2′-biphenyl; **k** Me, Me, H, $R^4 = Pr^i$ [a bis(bidentate ligand) complex]. [c] Angle θ.

escence of the crystal solvent in **1***, **1^*_{Me}**, **2***, **4*** and **6*** (see Table 1) it has not been included in the calculations of moments for these complexes. Complexes **7*** and **8*** are high spin in the solid state and in $(CD_3)_2SO$, while the remaining complexes with less bulky tetramethylene linkages are low spin. With the exception of **3***, the magnetic moments of **1***–**6*** are too small to be measured with confidence by the Evans method[7] in the spectrometer available for this purpose (200 MHz). A spin-equilibrium process is, however, obvious from the temperature-dependent ^{1}H NMR spectra; the paramagnetic shifts increase with temperature as the high-spin form is populated. Plots of chemical shifts *vs.* $1/T$ for complexes **1***–**6*** display the same

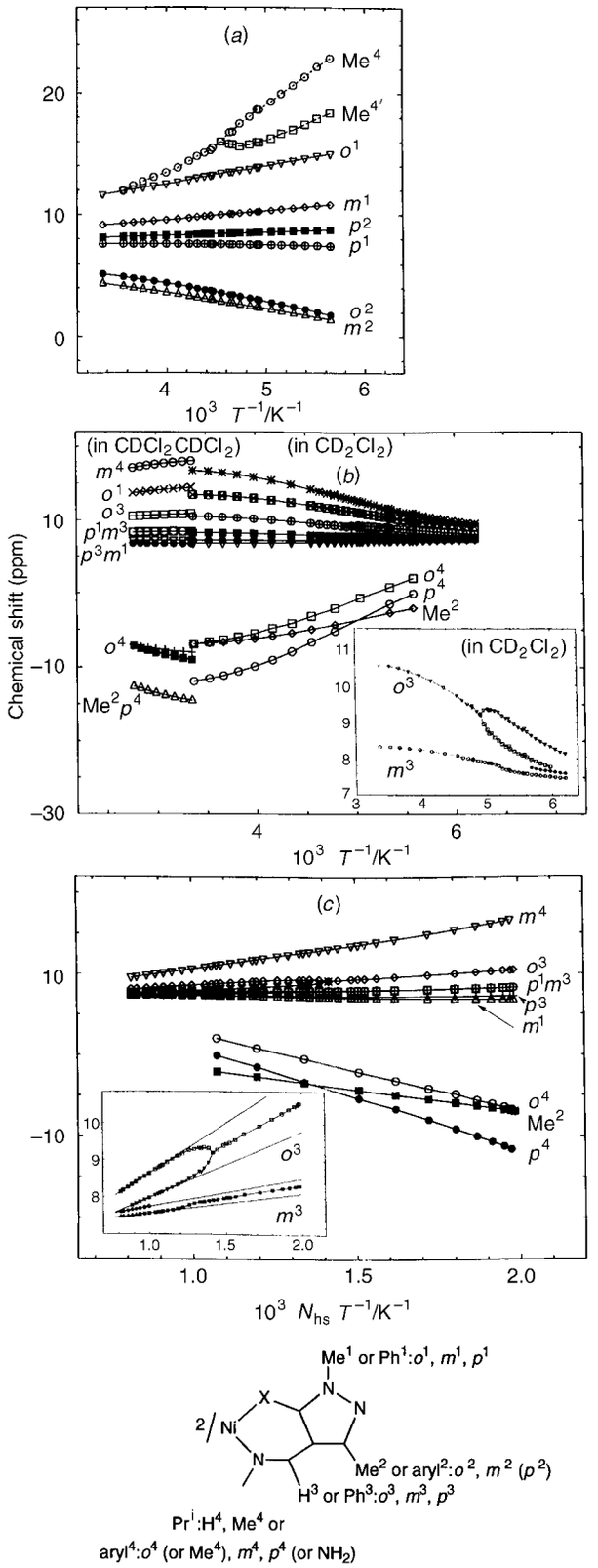

Fig. 3 Plots of the variable-temperature 400 MHz ^{1}H NMR spectra *vs.* $1/T$ for (*a*) complex **1** (in CD_2Cl_2), (*b*) **8** (in CD_2Cl_2 and in $CDCl_2CDCl_2$) and (*c*) **8** *vs.* N_{hs}/T (in CD_2Cl_2). The plots for the diastereotopic protons are shown in the insets; $\Delta\nu^0(T)$ used to calculate the rate constants for the racemization process (see Experimental section and below) for each pair of protons at every T is the vertical distance between the linear plots shown in (*c*), inset

behaviour as that for **8** [Fig. 3(*b*)] in contrast with the Curie-law dependence similar to that for **1** [Fig. 3(*a*)] for **7*** and **8***, measured from 25 (**7***) or −50 (**8***) to 90 °C.

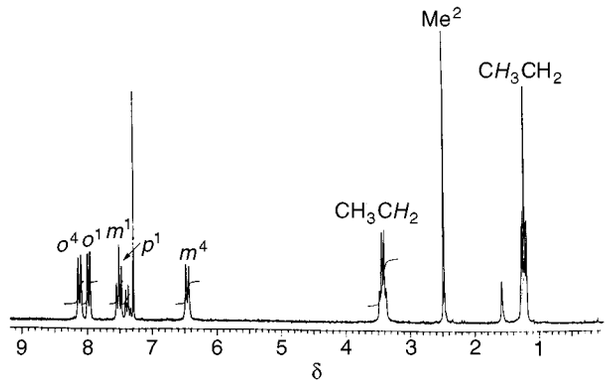

Fig. 4 The 200 MHz ^{1}H NMR spectrum of complex **11** measured in $CDCl_3$ at 25 °C. Chemical shifts for complex **10** measured under the same conditions are δ 8.06 (o^4), 7.95 (o^1), 7.53 (m^1), 7.44 (p^1), 7.25 (m^4, p^4) and 2.45 (Me^2)

Thermodynamic parameters for the spin-equilibrium process

The temperature-dependent chemical shifts for an indicator proton H_{ind} and an estimated coupling constant A_{ind} between H_{ind} and the unpaired spin density were used to determine N_{hs} and the equilibrium constants $K = N_{hs}/(1 - N_{hs})$ for the spin-equilibrium process (1) using the equation for the isotropic contact shift[9] [see Experimental section, equation (4)]. Thermodynamic parameters [Table 5(*a*) and 5(*b*)] were derived from the van't Hoff plots [Fig. 5(*a*) and 5(*b*)]. The reliability of the parameters was evaluated from the linear plots of the chemical shifts *vs.* N_{hs}/T [see Fig. 3(*c*)][4b] as described in the Experimental section. The parameters for complexes **2** and **9** [Table 5(*a*)] are derived from the linear plots obtained from −60 °C.

Complexes 1–6 (R^4 = Pr^i). For these complexes the spin state in solution is dependent on X and on the substituents on the pyrazolyl groups [see Table 5(*a*) and above]. A high-spin complex is obtained when X = NH (**1**) or, in the case of X = S, when one or both substituents are aliphatic (**3**–**6**); a spin-equilibrium system is obtained when X = S and both substituents are aromatic (**2**).

An explanation for the effect of the donor atom X and of pyrazolyl substitution on the spin state may be found in the ligand-field parameters derived from the electronic spectra (see below).

Complexes 7–9 (R^4 = aryl). It is seen [Table 5(*a*) and above] that aryl substitution of the nitrogen donor atoms favours the low-spin state more than does alkyl substitution. The relatively favourable conditions for the existence of a planar low-spin population in **8** and **9** may be due to coplanarity of the aromatic rings on the nitrogen-donor atoms with the chelate rings; just such a structure was observed for a similar nickel(II) complex.[11] This would permit a close packing of the aromatic rings and a relatively small[6a] distortion from a *cis*-planar co-ordination geometry. The angle θ is 68.7° in the complex presented in ref. 11.

The existence of a low-spin population for complex **7** is attributed mainly to steric effects from the 2,6-$Me_2C_6H_3$ rings. In crystal structures[4d,10] of similar $M^{II}N_2S_2$ complexes these rings are orthogonal to the plane of the chelate rings, and the complexes are forced towards *trans*-planar co-ordination geometries, probably due to the steric bulk of the xylyl rings. Nickel(II) N_2O_2 complexes of the salicylaldimine type strongly associate forming paramagnetic six-co-ordinated Ni^{II} in the solid state and in solution if the substituents on the nitrogen-donor atoms are *meta*- or *para*-substituted phenyl in contrast with complexes that have *ortho*-substituted phenyl in these positions.[12,13] This is attributed to steric effects from the *ortho*-

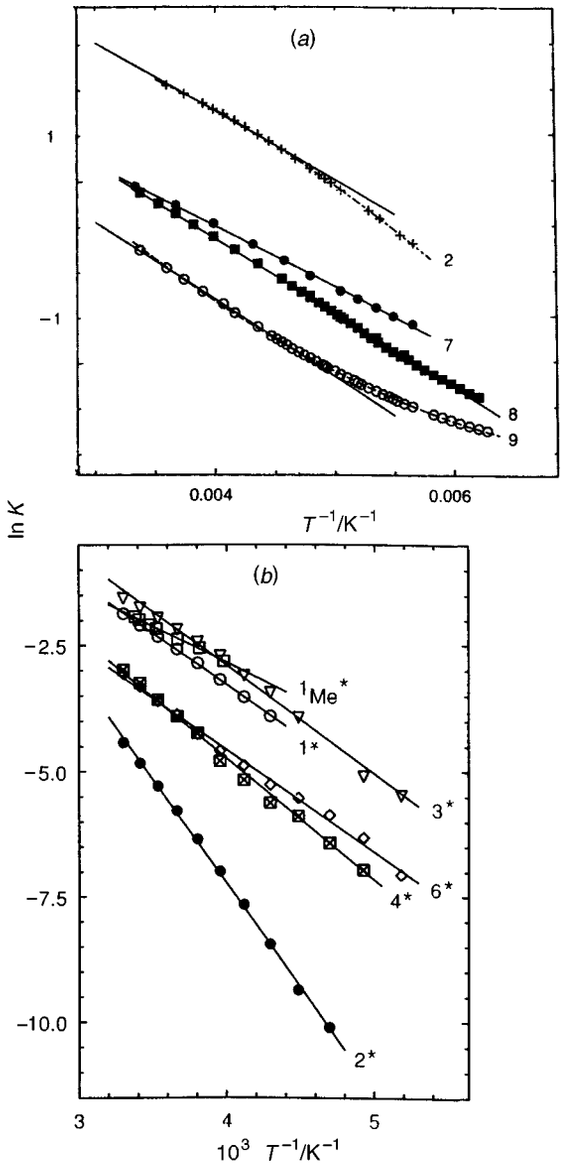

Fig. 5 Van't Hoff plots for the spin-equilibrium process of (*a*) the bis(bidentate ligand) complexes, (*b*) the tetradentate ligand complexes in CD_2Cl_2

substituted phenyl rings which are presumed to be orthogonal to the chelate rings both in the solid state and in solution.[12,13]

Fully paramagnetic bis(bidentate ligand)nickel(II) N_2X_2 Schiff-base complexes incorporating pyrazole have been known for more than a decade.[6a] A single complex prepared recently[10] was found to be low spin in the solid state and in spin equilibrium in solution [$\mathbf{7}_{\mathbf{diPh}}$, Table 5(*a*)]. Our investigations show that several ligand modifications may stabilize the low-spin form of pyrazole-based bis(bidentate ligand) complexes.

In general nickel(II) N_2X_2 Schiff-base complexes incorporating aromatic carbon rings (benzene, naphthalene) or β-ketoamines have a greater tendency to be low spin than the complexes incorporating a heterocyclic aromatic ring[6a] (*e.g.* pyrazole[1c,4c,6a] and isoxazole[4b]). This may be due to the inductive effect of the heteroatoms in the latter cases.[1c] The thermodynamic parameters for the spin-equilibrium systems listed in Table 5(*a*) show that the low-spin state is less favoured in the present complexes than in most bis(bidentate ligand) N_2S_2 Schiff-base complexes incorporating β-thioketoamines[14a] and benzene.[6a,14b,c] To our knowledge the complexes of the latter type are low spin in the solid state and in solution[14b] with few exceptions (a Bu^t substituent on the nitrogen-donor atom results in a fully paramagnetic complex,[14b,c] while a Bu^n substituent results in a spin-equilibrium system[6a]). Schiff-base N_2S_2 ligands incorporating cyclopentene seem also to favour the low-spin state more than do the pyrazole-based ligands.[14d]

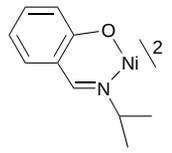

n[15]

Complexes with tetradentate ligands. The thermodynamic parameters for the tetradentate ligand complexes measured in different solvents are given in Table 5(*b*). As seen in the bis(bidentate ligand) complexes and in previous studies,[4c,5f] pyrazolyl diaryl substitution tends to stabilize the low-spin state compared with dialkyl or alkylaryl substitution. Comparisons of $N_2(NH)_2$ and N_2S_2 complexes with equivalent pyrazolyl substitution (**1*** and $\mathbf{1_{Me}}$* *vs.* **2*** and **5***) show that the low-spin state is most favoured when X = S as also seen in the bis(bidentate ligand) complexes described above (**1** *vs.* **2**). Thermodynamic parameters measured in $CDCl_3$ for complex **1***[4a] and for $n = 4$ N_2S_2 complexes[1c,6b] similar to **2***–**6*** are listed in Table 5(*b*) for comparison (structures **h***–**j*** and **l***, **m***, see Table 5, footnote). Reported values[6b] for complex **h*** are unusually low and have been redetermined [see Table 5, footnote]. As observed for other systems[14a] the spin-equilibrium process is strongly dependent on the solvent. The concentration of low-spin molecules seems to be correlated with the dipole moment μ of the solvent. The solvents favour N_{hs} in the order $(CD_3)_2SO$ (μ = 3.96) < CD_2Cl_2 (1.57) < $CDCl_2CDCl_2$ (1.3) < $CDCl_3$ (1.1 D) possibly due to a stronger solvation of the metal centre in the low-spin form by the more polar solvents.[2c] Thermodynamic parameters for the N_2S_2 complexes **2***–**6*** could not be derived in $(CD_3)_2SO$ using the above method. A resonance not seen in the $CDCl_2CDCl_2$ spectra indicates that new species are formed involving co-ordinated $(CD_3)_2SO$. The ability to take up co-ordinating solvent is also observed in the electronic spectra of the tetradentate ligand N_2S_2 complexes in Me_2SO, but not in the NMR or electronic spectra of the bis(bidentate ligand) complexes, of the tetradentate ligand $N_2(NH)_2$ complexes or of the tetradentate ligand N_2S_2 high-spin complexes.

Electronic spectra; ligand–field parameters

Electronic spectral data measured in $CHCl_3$ are given in Table 6. T_d Symmetry is assumed for the Schiff-base complexes, and the ligand-field transitions for the bis(bidentate ligand) complexes and for the tetradentate ligand high-spin complexes **7*** and **8*** were identified by comparison with the spectrum of complex **n**;[15a] the assignments of ref. 4(*b*) for complex **5*** were used for the tetradentate ligand spin-equilibrium systems **1***–**6***. Charge transfer (c.t.) and intraligand transitions were identified from the intensities [see also ref. 4(*b*) for the assignments of c.t. transitions of the N_2S_2 complexes **2***–**6***].

Ligand-field parameters (Table 7) were derived for the Schiff-base complexes by the method described in the Experimental section. Ligand-field parameters[1c] for the biphenyl-bridged spin-equilibrium systems (**l*** and **j***), pyrazolyl substituted as complexes **3** and **4**, respectively, are listed in Table 7 for comparison. Comparisons of $N_2(NH)_2$ and N_2S_2 complexes show that the magnitudes of the ligand field, Δ_{T_d}, are larger for the former, probably due to the strong Lewis basicity of the aminato function (reflected in the magnitude of e_σ). The larger ligand-field strengths for the N_2S_2 complexes (reflected in the magnitude of Δ_{T_d}/B, where B is the Racah parameter) is due to a more reduced interelectronic repulsion on the nickel(II) ion (reflected in the smaller value of B).‖ Within the N_2S_2 series low

‖ Our results are consistent with the expectations of lower values of B in systems with soft donor atoms (*e.g.* S and P) than in systems with hard donor atoms (*e.g.* N).[16]

Table 4 Magnetic moments

(*a*) Bis(bidentate ligand) complexes

	1	**2**	**3**	**6**	**7**	**8**	**9**	$[Cr^{III}(acac)_3]$ [a]
μ/μ_B [b]	3.13	3.01	3.19	3.22	0.90	1.06	1.08	
μ/μ_B [c]	3.43(6)	3.20(8)	3.31	3.32(2)	3.05(2)	3.12(3)	2.25(12)	3.99(3)
Change [d]	−2	3	0	−2	5	6	20	−2

(*b*) Tetradentate ligand complexes

	1*	**2***	**3***	**4***	**5***	**6***	**7***	**8***
μ/μ_B [e]	1.01(6)	0.95(8)	1.04(5)	1.10(3)	0.96(10)	1.02(11)	3.24(2)	3.23(8)
μ/μ_B [f]	—	—	1.97(5)	—	—	—	3.30	3.24

[a] A paramagnetic standard measured under the same conditions. [b] Measured in the solid state at 22 °C. The solid-state moments for complexes **4**, **5**, **10** and **11** are 3.11, 3.25, 0.92 and 1.05 μ_B, respectively. [c] Measured in $(CD_3)_2SO$ at 25 °C by the Evans method. [d] Change (%) of moment from 25 to 90 °C. [e] Measured in the solid state at 24 °C. [f] Measured as in *c*; complex $\mathbf{1_{Me}}$* was not measured due to lack of material.

Table 5 Thermodynamic parameters for the spin-equilibrium process of the complexes

(*a*) Bidentate ligands

Complex	ΔH/kJ mol^{-1}	ΔS/J K^{-1} mol^{-1}	ΔG_{25}/kJ mol^{-1}	K_{25}	Correlation coefficient [a]
2 [b]	6.26 ± 0.28	35.5 ± 1.1	−4.32 ± 0.05	5.72 ± 0.12	0.9988
2 [c]	4.02 ± 0.42	32.3 ± 1.3	−5.61 ± 0.03	9.56 ± 0.13	0.9956
7 [b]	5.58 ± 0.15	22.2 ± 0.7	−1.04 ± 0.06	1.52 ± 0.04	0.9996
$\mathbf{7_{diPh}}$ [d]	11.80 ± 0.1	34.6 ± 1	1.48	0.55	
8 [b]	6.80 ± 0.17	25.9 ± 0.8	−0.92 ± 0.07	1.46 ± 0.04	0.9994
9 [b]	7.12 ± 0.10	21.5 ± 0.4	0.71 ± 0.02	0.76 ± 0.01	0.9999

(*b*) Tetradentate ligands

1* [b]	17.0 ± 0.4	40.8 ± 1.5	4.84 ± 0.02	0.141 ± 0.001	0.9998
1* [c]	10.1 ± 0.3	17.2 ± 0.9	4.97 ± 0.03	0.137 ± 0.002	0.9996
1* [e]	21.5 ± 0.9	41.3 ± 2.8	9.23 ± 0.08	0.024 ± 0.001	0.9993
1* [d]	8.8 ± 0.1	25.1 ± 4.2	1.3 ± 0.1	0.59 ± 0.03	
$\mathbf{1_{Me}}$* [b]	12.1 ± 0.6	24.6 ± 2.2	4.80 ± 0.08	0.149 ± 0.005	0.9990
$\mathbf{1_{Me}}$* [c]	11.2 ± 0.2	22.7 ± 0.6	4.45 ± 0.02	0.166 ± 0.001	0.9999
$\mathbf{1_{Me}}$* [e]	21.8 ± 0.5	36.2 ± 1.5	11.01 ± 0.04	0.012 ± 0	0.9998
2* [b]	34.5 ± 1.1	77.8 ± 4.5	11.31 ± 0.22	0.011 ± 0.001	0.9995
2* [c]	19.3 ± 0.5	32.6 ± 1.4	9.58 ± 0.04	0.021 ± 0	0.9998
3* [b]	17.8 ± 1.3	47.2 ± 5.5	3.72 ± 0.34	0.022 ± 0.003	0.9972
3* [c]	12.0 ± 0.6	26.3 ± 1.7	4.14 ± 0.05	0.188 ± 0.004	0.9991
l* [d]	9.56	23.7	2.63	0.340	
i* [d]	8.26	21.7	1.90	0.459	
4* [b]	20.1 ± 1.7	41.1 ± 7.2	7.85 ± 0.40	0.042 ± 0.007	0.9961
4* [c]	15.0 ± 0.5	28.7 ± 1.4	6.44 ± 0.04	0.073 ± 0	0.9996
j* [d]			5.70	0.096	
m* [d]	11.7	23.4	4.86	0.137	
5* [b]	15.8 ± 0.3	26.8 ± 1.1	7.80 ± 0.1	0.043 ± 0.010	0.9997
5* [c]	14.9 ± 0.5	24.4 ± 1.4	7.59 ± 0.04	0.047 ± 0.001	0.9996
6* [b]	16.9 ± 1.2	29.7 ± 4.9	8.05 ± 0.31	0.039 ± 0.001	0.9975
6* [c]	14.7 ± 0.8	23.1 ± 2.3	7.74 ± 0.07	0.044 ± 0.001	0.9989
h* [d]	14.2 ± 0.4	30.6 ± 1.8	5.08 ± 0.09	0.128 ± 0.004	0.9997

E.s.d.s were calculated as described in ref. 4(*b*). Complex $\mathbf{7_{diPh}}$, is a pyrazolyl 1,3-diphenyl-substituted bis(bidentate ligand) complex[10] analogous to **7**. The tetradentate ligand complexes **l*** and **j*** are biphenyl-bridged and pyrazolyl-substituted as **3*** and **4***, respectively, and **i*** and **m*** are the corresponding 6,6′-dimethylbiphenyl-bridged complexes.[1c] Complex **h*** is a pyrazole-based $n = 4$ complex $[R^1 = Pr^i, R^2 = Me, R^3 = (CH_2)_4]$.[6b] The parameters were calculated from the reported proton spectra of **h*** using equation (4); Me^2 was used as indicator group with $A = 0.305$ MHz, $B = 0$ and $\delta_{dia} = 2.4$. Literature values for **h*** are 2.1 kJ mol^{-1} and 6 J K^{-1} mol^{-1} for ΔH and ΔS, respectively.[6b] [a] Of the van't Hoff plot. [b] Measured in CD_2Cl_2 from −60 (complexes **2** and **9**), from −95 (**7**), from −110 (**8**), from −40 (**1***), from −22 ($\mathbf{1_{Me}}$*), from −60 (**2***) from −70 (**4***) and from −80 °C (**3*** and **6***) to about room temperature. [c] Measured in $CDCl_2CDCl_2$ from 25 to 90 °C. [d] Measured in $CDCl_3$. [e] Measured in $(CD_3)_2SO$ from 25 to 90 °C.

values of B are partly responsible for the larger ligand-field strengths of the aryl-substituted complexes.

Large values of Δ_{T_d}/B and of ΔH for the spin-equilibrium process are indicative of electronic stabilization of the low- relative to the high-spin state. For that reason the reliability of the ligand-field parameters for the spin-equilibrium systems may be evaluated from a plot of Δ_{T_d}/B *vs.* ΔH, see Fig. 6. The 95% probability interval is shown.

Kinetic parameters for the racemization process

Rate constants for the racemization process were derived from the temperature-dependent chemical shifts of diastereotopic protons, and values for the activation parameters (Table 8) were derived from the Eyring plots. The method described in ref. 2(*c*) was used unmodified for the fully paramagnetic complexes and with the modifications described in ref. 4(*b*) for the spin-equilibrium systems (see Experimental section).

Complexes with bidentate ligands. Previous NMR investigations of the racemization rates at the coalescence temperature T_c for pyrazole-based nickel(II) N_2S_2 Schiff-base complexes with alkyl-substituted nitrogen-donor atoms showed that the rate constants were independent of the concentration.[2b] This implies that the reaction mechanism is intramolecular for this type of complex and thus first-order kinetics would be expected for complexes **2**–**6**. Similarly, in the present study the rate was

Table 6 Electronic spectra[a]

(*a*) Complexes with bidentate ligands

1	1457 (37),[b] 1290 (sh) (30),[c,*] 976 (15),[d] 650 (sh) (125),[e] 610 (sh) (180),[e,*] 575 (sh) (350),[e] 460 (sh) (3000),[f] 419 (4400),[f] 274 (57 000),[g] 260 (sh) (85 700)[g]
2	1500 (33),[b] 1330 (sh) (29),[c,*] 1200 (sh) (23),[d] 673 (455),[e,*] 509 (3370),[f] 430 (sh) (2710),[f] 300 (sh) (32 500),[g] 280 (sh) (44 200),[g] 250 (52 500)[g]
3	1575 (31),[b] 1345 (sh) (26),[c,*] 1200 (sh) (19),[d] 664 (415),[e,*] 505 (3490),[f] 400 (sh) (1730),[f] 320 (sh) (14 700),[g] 293 (18 600),[g] 280 (sh) (17 100),[g] 276 (20 000)[g]
4	1530 (37),[b] 1315 (sh) (33),[c,*] 1200 (sh) (25),[d] 669 (495),[e,*] 506 (3620),[f] 430 (sh) (2000),[f] 295 (sh) (31 900),[g] 280 (33 400),[g] 240 (sh) (34 000)[g]
5	1575 (34),[b] 1330 (sh) (29),[c,*] 1200 (sh) (22),[d] 665 (450),[e,*] 508 (3075),[f] 400 (sh) (2310),[f] 300 (23 100),[g] 250 (46 000)[g]
6	1570 (34),[b] 1330 (sh) (29),[c,*] 1200 (sh) (20),[d] 666 (420),[e,*] 508 (3430),[f] 400 (sh) (2800),[f] 301 (26 800),[g] 243 (56 500)[g]
7	1920 (52),[b] 1322 (31),[c,*] 1210 (27),[d] 715 (360),[e,*] 585 (sh) (600),[f] 500 (sh) (1170),[f] 410 (6500),[f] 325 (18 900)[g]
8	1790 (40),[b] 1340 (38),[c,*] 1175 (sh) (30),[d] 720 (650),[e,*] 499 (2070),[f] 420 (sh) (3710),[f] 375 (sh) (7190),[g] 325 (sh) (18 950)[g]
9	714 (560),[e] 540 (sh) (1230),[f] 495 (sh) (2040),[f] 400 (sh) (7920),[f] 330 (sh) (21 330)[g]
10	690 (sh) (310),[h] 540 (sh) (3170),[f] 364 (30 500)[g]
11	690 (sh) (760),[h] 520 (sh) (17 950),[f] 462 (25 800),[g] 353 (18 900)[g]

(*b*) Complexes with tetradentate ligands

1*	1700 (12),[b] 1143 (21),[c,*] 1025 (15),[d] 635 (sh) (155),[e] 585 (sh) (220),[e] 485 (sh) (740),[f] 396 (5060),[f] 325 (sh) (21 800),[g] 280 (sh) (53 500),[g] 261 (62 400)[g]
1_{Me}*	1790 (6),[b] 1158 (11),[c,*] 1037 (7),[d] 640 (sh) (110),[e] 580 (sh) (165),[e] 480 (sh) (710),[f] 396 (4660),[f] 325 (sh) (11 700),[g] 280 (29 500)[g]
2*	1700 (3),[b] 1280 (4),[c,*] 644 (163),[d] 510 (sh) (245),[f] 420 (sh) (1995),[f] 365 (7080),[g] 303 (64 100),[g] 295 (sh) (43 000),[g] 256 (81 200)[g]
3*	1825 (8),[b] 1237 (13),[c,*] 683 (198),[e,*] 542 (545),[f] 420 (1950),[f] 360 (sh) (4960),[g] 295 (25 200),[g] 266 (42 400)[g]
4*	1800 (4),[b] 1223 (6),[c,*] 663 (sh) (140),[e] 540 (sh) (335),[f] 425 (1960),[f] 360 (sh) (5750),[g] 293 (33 800),[g] 263 (34 400)[g]
6*	1780 (4),[b] 1230 (6),[c,*] 654 (209),[e] 530 (sh) (310),[f] 410 (sh) (2430),[f] 355 (sh) (8510),[g] 301 (43 900)[g]
7*	1676 (64),[b] 1360 (sh) (40),[c,*] 1192 (30),[d] 890 (sh) (60),[d] 716 (385),[e,*] 545 (sh) (985),[f] 475 (1910),[f] 420 (sh) (1700),[f] 332 (10 900)[g]
8*	1600 (59),[b] 1370 (sh) (43),[c,*] 1240 (21),[d] 865 (sh) (40),[d] 710 (320),[e,*] 535 (sh) (900),[f] 472 (1850),[f] 340 (sh) (9 250)[g]

[a] Measured in $CHCl_3$ at room temperature; wavelengths are quoted in nm, absorption coefficients (in parentheses) in $dm^3\ mol^{-1}\ cm^{-1}$; sh = shoulder; T_d symmetry has been assumed for the Schiff-base complexes, the ground state is $^3T_1(F)$; D_{4h} symmetry has been assumed for the aza complexes, the ground state is $^1A_{1g}$. Transitions marked with an asterisk were used in the calculations of ligand-field parameters (see Table 7). The ligand-field and charge-transfer transitions for **2**–**6** were presented in part in ref. 2(*c*), but quoted wrongly for **2**; λ_{max} of $^3A_2(F)$ for **1**–**6**, **7*** and **8*** is estimated to lie at the average energy of the first observed transition and the shoulder at about 1360 nm. [b] Superposition of high-energy components of $^3T_2$ (F) split by spin–orbit coupling and low symmetry. [c] $^3A_2(F)$. [d] Spin-forbidden singlet transition. [e] Component of $^3T_1(P)$. [f] Charge-transfer transition. [g] Intraligand transition. [h] $^1A_{2g}$.[4c,5f]

found to be independent of the concentration for complexes **1**, **8** and **9**, which were investigated at 5.8 and 11.6, 5.8 and 12.2 and 4.8 and 8.3 mg cm^{-3}, respectively. It has been shown that racemization mainly *via* a twist mechanism without bond rupture is most probable for complexes **4**–**6**.[2c] The activation parameters listed in Table 8 are consistent with this type of mechanism in every case.

The kinetic studies described in ref. 2(*b*) were limited to the different coalescence temperatures for different indicator protons, which complicates reliable comparisons within this series and with the present series. However, our results are consistent with those reported in ref. 2(*b*). Coalescence temperatures were less than 0 °C and values of $\Delta G^{\ddagger}_{T_c}$ were in the range 41.4–55.6

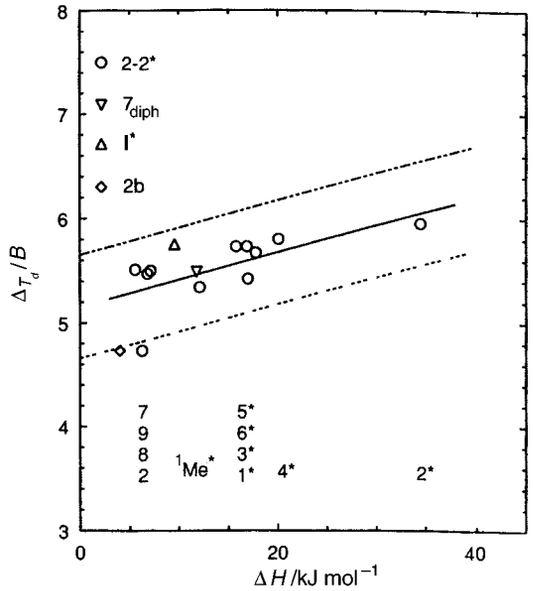

Fig. 6 Plots of Δ_{T_d}/B in $CHCl_3$ *vs.* ΔH for the spin-equilibrium process in CD_2Cl_2 (circles); the complex numbers are, from top to bottom, given in the same order as the circles plotted within clusters of similar enthalpies; $\Delta_{T_d}/B = 5.5$ has been estimated for complex **9**. Values of ΔH for $\mathbf{7}_{diPh}$ and **1*** were measured in $CDCl_3$;[1c,10] **2b** represents the value of ΔH for complex **2** measured in $CDCl_2CDCl_2$

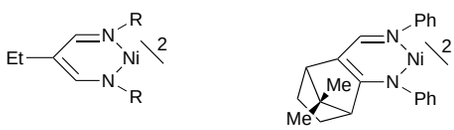

o R = Me[17a]
p R = Ph[2a]
q[17b]

kJ mol^{-1}, except for the complexes with Bu^t-substituted nitrogen donor atoms (T_c 60–100 °C, $\Delta G^{\ddagger}_{T_c}$ 70.7–73.6 kJ mol^{-1}).[2b]

The racemization kinetics of the pseudo-tetrahedral nickel(II) $N_2(NR)_2$ complexes of the type represented by structures **o**–**q** have been studied extensively.[2a,17] The rate law is first order, and it has been shown by ligand-exchange experiments that racemization, at least partly, *via* an intramolecular bond-rupture/bond-reassociation mechanism is probable.[17b,c] The activation parameters for complexes **o**–**q** are listed in Table 8 for comparison with the $N_2(NH)_2$ complex **1**. The larger configurational stability of **o**–**q** is due mainly to the larger activation enthalpies, which are consistent with a mechanism involving the breaking of bonds. However, the negative activation entropies for **o** and **q** investigated in non-co-ordinating solvent indicate that a twist mechanism may also be of some importance for this type of complex.

Despite the fact that racemization is expected to occur *via* a planar four-co-ordinate activated complex for the bis(bidentate ligand) complexes presented in ref. 2(*c*) and for those in this work, a correlation is not found between the tendency to be planar and low spin (reflected in the thermodynamic parameters for the spin-equilibrium process and in the ligand-field parameters) and the racemization rate. Other aspects, mainly steric effects, are more important. Bulky substituents on the imine nitrogen atoms such as Bu^t slow down the racemization.[2b] A correlation has been found, however, between the co-ordination geometry in the solid state and $\Delta G^{\ddagger}_{T_c}$.[13] A decreasing angle θ increases the racemization rate[13] indicating that the preferred co-ordination geometry of the activated complex is *cis*. The very fast racemization for complex **7** ($T_c < -95$ °C was not observed for the diastereotopic groups, Me^4)** may be due

** The Me^4 groups are seen to be diastereotopic in the zinc(II) complex analogous to complex **7** ($T_c > 130$ °C in $CDCl_2CDCl_2$).[4d]

Table 7 Ligand-field parameters[a]

	Bidentate ligands						Tetradentate ligands				
Complex	B	Δ_{T_d}	e_σ	e_π	Δ_{T_d}/B	Complex	B	Δ_{T_d}	e_σ	e_π	Δ_{T_d}/B
1	910	3975	3835	640	4.37	**1***	873	4740	4570	760	5.42
n	750	3805	4000	860	4.42	$\mathbf{1_{Me}}$*	876	4675	4510	750	5.34
2	815	3855	3335	335	4.73	**2***	753	4480	3875	385	5.95
3	835	3770	3265	325	4.51	**3***	773	4385	3795	380	5.67
4	820	3840	3325	335	4.68	**l*** [1c]	770	4420			5.74
5	835	3770	3265	325	4.51	**3***	794	4105	3550	355	5.17
6	830	3775	3265	325	4.55	**4***	763	4425	3830	385	5.80
7	743	4095	3545	355	5.51	**j*** [1c]	770	4570			5.87
8	739	4040	3495	350	5.47	**5***	769	4405	3810	380	5.73
						6*	768	4400	3810	380	5.73
						7*	765	3615	3130	315	4.73
						8*	770	3680	3185	320	4.78

[a] Calculated from the electronic absorption spectra in $CHCl_3$ at room temperature (Table 6); energies are in cm^{-1}. Complex **n** is high spin in the solid state,[15a] but in spin equilibrium in solution;[15b] its ligand-field parameters in the solid state were presented in ref. 15(*a*). The value for B was estimated; average values for $e_{\sigma O}$ and $e_{\sigma N}$, and for $e_{\pi O}$ and $e_{\pi N}$ are listed here. The electronic spectra of complex **5*** were presented in ref. 4(*b*).

Table 8 Kinetic parameters for the racemization process[a]

(*a*) Complexes with bidentate ligands

	$\Delta H^\ddagger$/kJ mol^{-1}	$\Delta S^\ddagger$/J K^{-1} mol^{-1}	$\Delta G^\ddagger_{25}$/kJ mol^{-1}	k_{25}/s^{-1}	Correlation coefficient[b]	T_c[c]/ °C
1	8.80 ± 1.59	−136 ± 8	49.4 ± 0.7	(1.4 ± 0.4) × 10^4	0.9837	−55
o [17a]	25 ± 8	−126 ± 42	63 (78)[d]	56 (1.7 × 10^3 [d])		85
p [2a]			(91)[d]	(42[d])		147
q [17b]	94 ± 3	−63 ± 3	113 (120)[d]	≈0 (11[d])		
2	21.5 ± 2.7	−88.3 ± 12.0	47.8 ± 0.8	(2.6 ± 0.8) × 10^4	0.9949	−33
3	32.3 ± 3.2	−70.3 ± 11.0	53.3 ± 0.2	(3.0 ± 0.3) × 10^3	0.9956	−19
4 [2c]	34.6	−56.7	51.5	5.8 × 10^3		0
5 [2c]	26.5	−75.6	49.0	1.6 × 10^4		−24
6 [2c]	11.1	−144	54.0	2.2 × 10^3		−54
8 [e]	30.5 ± 1.9	−33.4 ± 9.8	40.5 ± 1.0	(5.3 ± 2.1) × 10^5	0.9937	−70
9	35.0 ± 1.6	−22.3 ± 7.7	41.7 ± 0.7	(3.2 ± 0.8) × 10^5	0.9986	−62

(*b*) Complexes with tetradentate ligands

1*	27.8 ± 5.8	−63.1 ± 27.1	46.6 ± 2.2	(5.1 ± 4.0) × 10^4	0.9900	≈−55
$\mathbf{1_{Me}}$*	35.9 ± 2.2	−35.3 ± 9.5	46.5 ± 0.7	(4.7 ± 1.3) × 10^4	0.9985	≈−40
3*	51.9 ± 5.8	5.9 ± 21.0	50.1 ± 0.6	(1.0 ± 0.2) × 10^4	0.9962	0
4*	50.0 ± 6.1	−4.2 ± 23.9	51.2 ± 1.0	(6.8 ± 2.6) × 10^3	0.9966	≈−10
5* [4b]	50.5 ± 2.7	5.5 ± 9.9	48.9 ± 0.2	(1.7 ± 0.2) × 10^4	0.9981	4
6*	48.2 ± 5.0	−4.9 ± 19.5	49.7 ± 0.8	(1.2 ± 0.3) × 10^4	0.9976	−20
7*	47.8 ± 5.5	−51.5 ± 16.2	63.1 ± 0.7	54 ± 15	0.9932	72
8*	40.4 ± 7.4	−67.3 ± 22.4	60.5 ± 0.7	159 ± 44	0.9839	56

[a] Measured in CD_2Cl_2 (complexes **o**–**q**,[2c,17a,b] **7*** and **8*** in $CDCl_2CDCl_2$); e.s.d.s were calculated as described in ref. 4(*b*). [b] Of the Eyring plots. [c] The coalescence temperatures are dependent on the indicator protons and on the spectrometer frequency and are not directly comparable. [d] At 147 °C. [e] Indicator is *o*[3]; with *m*[3] as indicator the values 30.7 kJ mol^{-1}, −37.3 J K^{-1} mol^{-1} and 41.8 kJ mol^{-1} were calculated for $\Delta H^\ddagger$, $\Delta S^\ddagger$ and $\Delta G^\ddagger_{25}$, respectively.

to a relatively uncrowded *trans*-planar transition state, in agreement with the crystal structures of similar metal(II) complexes[10] and the racemization kinetics observed for the analogous zinc(II) complex.[4d]

For complexes investigated in this work and in ref. 2(*c*) the variations may be explained partly by solvent effects; a relatively strong solvation of the planar transition state should yield a small value of $\Delta H^\ddagger$ and a strongly negative value of $\Delta S^\ddagger$. Based on the relative values of $\Delta H^\ddagger$, the extent of solvation increases in the order **9** ⩽ **4** ⩽ **3** ⩽ **8** < **5** < **2** < **6** ⩽ **1**, whereas based on relative values of $\Delta S^\ddagger$ it increases in the order **9** ⩽ **8** ⩽ **4** ⩽ **3** ⩽ **5** ⩽ **2** < **1** ⩽ **6**.

Complexes with tetradentate ligands. Recent investigations[4b] of complex **5*** showed that the racemization rate is independent of the concentration signifying an intramolecular reaction mechanism and first-order kinetics. First-order kinetics might thus be expected for the related N_2S_2 spin-equilibrium systems **2***–**4*** and **6***. Similarly, a concentration dependence was not observed for $\mathbf{1_{Me}}$*, **7*** and **8***, which were investigated at 4.0 and 7.0, 4.3 and 8.6, and 6.6 and 13.2 mg cm^{-3}, respectively. First-order kinetics is also expected for **1***, due to its similarity to $\mathbf{1_{Me}}$*. Most complexes were studied at 200 or 250 MHz; $\mathbf{1_{Me}}$* and **5*** [4b] were studied at 400 MHz, which is reflected in the smaller uncertainties of the parameters for these complexes (Table 8). The results are consistent within the three groups of related complexes: (*a*) the $N_2(NH)_2$ spin-equilibrium systems **1*** and $\mathbf{1_{Me}}$*, (*b*) the N_2S_2 spin-equilibrium systems **3***–**6***, and (*c*) the high-spin complexes **7*** and **8***.

A racemization mainly *via* a twist mechanism has been assumed for the tetradentate ligand Schiff-base complexes incorporating pyrazole.[4a,6] A twist mechanism implies a planar four-co-ordinate activated complex, and in systems with tetradentate ligands the activated complex will necessarily be *cis* and crowded. Consequently, strongly negative activation entropies must be expected, and such are found for the $N_2(NH)_2$ complexes **1*** and $\mathbf{1_{Me}}$* and for the high-spin complexes **7*** and **8***. The kinetic parameters for the four complexes are consistent with a racemization *via* the expected twist mechanism. In the case of **7*** and **8*** the large positive activation enthalpies may be

due to an elongation of the M–L bonds in a very crowded transition state as a result of the bulky tetramethyl-substituted linkage. Recently reported values of $\Delta G^{\ddagger}_{T_c}$ for complex **1*** measured in CD_2Cl_2 at 300 MHz (42.8 and 44.2 kJ mol^{-1} at −60 and −44 °C)[4a] are similar to those found for **1*** in the present experiment at these temperatures (41.2 and 42.2 kJ mol^{-1}).

For the N_2S_2 complexes **3***–**6*** †† the parameters are not consistent with a twist mechanism. Activation entropies close to zero and large activation enthalpies indicate that the racemization may take place at least partly *via* an intramolecular bond-rupture/bond-reassociation mechanism. The $n = 4$ N_2S_2 complex **h*** [see Table 3(*b*)] endures activation barriers at the coalescence temperatures ($\Delta G^{\ddagger}_{T_c} \approx 50$ kJ mol^{-1} at T_c −40 and −10 °C)[6b] similar to those obtained at these temperatures for complexes **3***–**6***.

Conclusion

The purposes of this work were (1) to find ligand modifications that might stabilize the low-spin state in chiral $Ni^{II}N_2X_2$ Schiff-base or aza complexes incorporating pyrazole in order (2) to investigate the influence of the spin state on the racemization process $\Delta \rightleftharpoons \Lambda$ in solution, and (3) to evaluate the mechanism(s) for this process further. The ^{1}H NMR spectra of two bis(bidentate ligand) aza complexes show that these are low spin and achiral. However, the Schiff-base complexes investigated have very different magnetic properties in solution and, as they are all pseudo-tetrahedral and chiral, were suitable for the comparative study (2).

Complexes with bidentate ligands. Previously reported results[2b] and our investigations [ref. 2(*c*) and this work] show that a twist mechanism *via* a four-co-ordinate planar activated complex is most probable for the bis(bidentate ligand) complexes for a number of reasons. The rate is independent of the concentration and the mechanism consequently intramolecular. Addition of the strong tetradentate pro-ligand *N*,*N*′-bis(salicylidene)ethane-1,2-diamine (H_2salen) to a solution of a nickel(II) complex results in slow ligand exchange, much slower than the rate of racemization.[2c] This result makes an intramolecular bond-rupture/bond-reassociation mechanism improbable. Investigations of the same complex in two non-co-ordinating solvents of different polarity show that an increase in the low-spin population and a simultaneous increase of the racemization rate at low temperature (due to a reduced $\Delta H^{\ddagger}$) take place in the more polar solvent.[2c] This indicates that the process follows a route in which the low-spin form is a necessary intermediate. The activation parameters [ref. 2(*c*) and this work], in particular strongly negative activation entropies and relatively small activation enthapies, are consistent with the proposed mechanism *via* a planar and crowded activated complex without breaking of bonds. Given these results, pathway (3) may be proposed for the racemization[2c] (subscripts ls and hs

$$\Delta_{hs} \rightleftharpoons \Delta_{ls} \rightleftharpoons \text{activated complex} \rightleftharpoons \Lambda_{ls} \rightleftharpoons \Lambda_{hs} \quad (3)$$

refer to the low- and high-spin form, respectively). A chirality has been assigned to the low-spin forms for steric reasons. If this mechanism is accepted our results require that the first step be fast and without any importance for the racemization kinetics, since a correlation is not found between the kinetic parameters and the spin state of the racemizing complex. The slower second step is rate determining, and the rate is controlled by the steric bulk and extent of solvation of the activated complex.

Complexes with tetradentate ligands. The racemization kinetics of tetradentate ligand complexes have been studied less. Solvent- or ligand-exchange experiments have so far not been carried out and most conclusions drawn here are based on the magnitudes of the kinetic parameters ($\Delta H^{\ddagger}$ and $\Delta S^{\ddagger}$) alone. Concentration experiments indicate that the mechanism for the racemization is intramolecular. The results are consistent within three groups of related complexes: (1) N_2S_2 high-spin complexes with bulky linkages, (2) $N_2(NH)_2$ spin-equilibrium systems and (3) N_2S_2 spin-equilibrium systems with an unsubstituted tetramethylene linkage. The twist mechanism implies a planar activated complex which will necessarily be *cis* and crowded in tetradentate ligand complexes, and large negative activation entropies are expected. The observed kinetics for the group (1) and (2) complexes is in harmony with this condition. In contrast, positive activation entropies and strongly positive activation enthalpies are expected for a mechanism involving breaking of bonds. The parameters for the group (3) complexes are in harmony with these conditions indicating that the racemization may take place, at least partly, *via* an intramolecular bond-rupture/bond-reassociation mechanism. Ligand-exchange experiments will, however, be necessary to substantiate further the possibility of these mechanisms.

Experimental

Materials

Most chemicals used for the preparations were reagent grade and commercially available. They were used as received. Solvents used for analytical purposes were spectroscopic grade.

Preparations

See Table 1 for analytical data and solvents for recrystallization. The N_2S_2 complexes **2**–**6**,[2c] **2***–**6*** and **7**–**11**[4b] and the protonated pro-ligands corresponding to **2***–**8***, **7**–**9**[4d] and **10** and **11**[3] were prepared according to literature methods. Complexes **7*** and **8*** could not be formed from pro-ligand and nickel(II) acetate in MeOH as described in ref. 4(*b*) and absolute EtOH was used instead.

Nickel(II) $N_2(NH)_2$ complexes 1, 1* and 1_{Me}*. The following general template procedure was used. A suspension of the appropriate *o*-aminopyrazolecarbaldehyde (3.8 mmol) prepared according to ref. 18 was stirred in absolute EtOH (7 cm^3). Isopropylamine (for **1**, 3.8 mmol) or 1,4-diaminobutane (for **1*** and $\mathbf{1_{Me}}$*, 1.9 mmol) and nickel(II) acetate tetrahydrate (1.9 mmol) were added. The mixture was heated to reflux temperature and stirred for 20 min under reflux. On cooling to room temperature the red (**1**) or dark green (**1*** and $\mathbf{1_{Me}}$*) solid was filtered off and washed with 96% EtOH on the filter.

Physical measurements

Proton NMR spectra of protonated pro-ligands and complexes in $CDCl_3$, CD_2Cl_2, $CDCl_2CDCl_2$ and $(CD_3)_2SO$ were obtained on Varian spectrometers (GEMINI 200 or Unity 400) or on a Bruker AC250P spectrometer provided with a VT1000 temperature controller; $SiMe_4$ was added as internal standard. Methanol was used for temperature calibration of the Varian spectrometers at low temperature (from −115 to 25 °C), ethylene glycol at high temperature (from 25 to 90 °C). The uncertainty in the temperature was 1°. Assignments for pro-ligands and complexes were accomplished by comparisons between similar systems and by selective decoupling of single protons. Temperature-dependent spectra of the complexes were collected from about −100 (**1** and **2**, **7**–**9** and **1***–**6***), from −65

†† We were not able to derive kinetic parameters for complex **2*** using the above method. Reliable corrections for the natural chemical shift differences between diastereotopic protons, strongly temperature-dependent in paramagnetic systems,[2c,4b] could not be obtained as the first indications of paramagnetism and of chemical exchange are observed in the spectra of the diastereotopic protons in the same temperature range.

(**3**), from −50 (**8***) or from 25 (**6** and **7***) to 90 °C. Electronic absorption spectra of the complexes in $CHCl_3$ were obtained in a 1 cm quartz cuvette on a thermostatted Shimadzu UV-3100 apparatus, electron-impact mass spectra on a Finnigan Mat SSQ710 or a Varian Mat 311A apparatus. Elemental analyses were performed at the H. C. Ørsted Institute, University of Copenhagen; the complexes were first dried for 24 h in vacuum at room temperature. Magnetic moments were measured at room temperature in the solid state on a Sherwood Scientific magnetic susceptility balance, and from 25 to 90 °C in $(CD_3)_2SO$ by the Evans method[7] with acetone as external and internal standard. Diamagnetic corrections were made using Pascal's constants.

Determination of thermodynamic parameters for the spin-equilibrium process

Equilibrium constants, $K = N_{hs}/(1 - N_{hs})$, for the spin-equilibrium process (1) were evaluated from the temperature-dependent chemical shifts for an indicator proton H_{ind}. The equation for the paramagnetic isotropic Fermi contact shift, $\delta_{i,iso}$, of H_i, equation (4),[9] was used in the form presented in ref.

$$\delta_{i,iso} = \delta_{i,obs} - \delta_{i,dia} = -[A_i\gamma_e hS(S + 1)10^6/3\gamma_H k]N_{hs}T^{-1} + B_i \quad (4)$$

2(*c*).‡‡ The coupling constant A_i §§ is in units of Hz (1 G = 2.8 MHz), $\delta_{i,obs}$ and $\delta_{i,dia}$ are the observed shift and the diamagnetic reference point (in ppm), B_i is the non-zero intercept[19b] (in ppm) and N_{hs} is the mole fraction of high-spin molecules. The other symbols have their usual meanings. For a high-spin complex ($N_{hs} = 1$) the plots of chemical shifts *vs.* $1/T$ for protons H_i yield straight lines (Curie-law dependence). In a spin-equilibrium system ($0 < N_{hs} < 1$) the substitution of A_i and B_i in equation (4) with estimated values of A_{ind} and B_{ind} for an indicator proton yields N_{hs} (and K). For the bis(bidentate ligand) complexes **2** and **7**–**9** ($N_{hs} > 10\%$ at −100 °C) good fits¶¶ for B_{ind} were obtained by transfer of this quantity from a similar high-spin complex. For the tetradentate ligand systems ($N_{hs} \approx 0$ at −100 °C) the best fits were obtained by assuming B_{ind} values of zero. Indicator protons and estimates of A_{ind} and B_{ind} are found in SUP 57244. The chemical shifts of the protonated proligands were used as the diamagnetic reference points, $\delta_{ind,dia}$, for **2**, **8** and **9**; the corresponding zinc(II) complex[4d] was used for **7**. The chemical shifts for the complexes at −100 (X = S) or at −110 °C (NH) were used as diamagnetic reference points for **1***–**6***, thus including the temperature-independent paramagnetism. For **1***–**6*** the chemical shifts are found to vary almost linearly with T at low temperature (with correlation coefficients >0.999). In the case of uncertain positions due to overlapping signals, the diamagnetic reference points were found by linear extrapolation from plots of $\delta_{ind,obs}$ *vs.* T at low temperature.

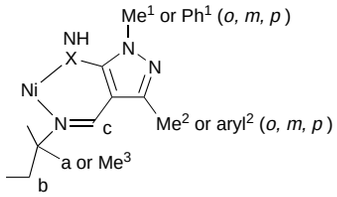

Derivation of angular overlap model ligand-field parameters

Ligand-field parameters were obtained from the electronic spectra (*a*) by assuming T_d symmetry and (*b*) by using the assignments of ref. 15(*a*) for the bis(bidentate ligand) complexes and the high-spin tetradentate ligand complexes **7*** and **8***, and (*c*) the assignment of ref. 4(*b*) for the tetradentate ligand spin-equilibrium systems **1***–**6***. The position of the $^3T_1(P)$ transition that is needed in the calculations[20] is uncertain for **1***–**6*** due to superposition with the $^1A_{2g}$ transition derived from low-spin complexes (D_{4h} is assumed).[4b] For **1*** and $\mathbf{1_{Me}}$* the transition energy $E[^3T_1(P)]$ for **1** has been estimated. In the case of X = S the energy of the superposition for the most paramagnetic of these tetradentate ligand spin-equilibrium systems, complex **3*** (N_{hs} 16% at 25 °C in $CDCl_2CDCl_2$), is $0.972E[^3T_1(P)]$ in the similarly pyrazolyl-substituted bis(bidentate ligand) complex **3** ($R^4 = Pr^i$). For **2*** and **4***–**6*** a similar lowering of the energy compared with that in **2** and **4**–**6** has been assumed. Methods in ref. 20 were used to derive the tetrahedral field Δ_{T_d} and the Racah interelectronic repulsion parameter B. The relation $\Delta_{T_d} = \frac{4}{9}(3e_\sigma - 4e_\pi)$[15a] was used to evaluate e_σ and e_π. The value of $e_\sigma/e_\pi = 6$, found for the $N_2(NH)_2$ complexes of ref. 5(*f*) to be independent of the tetrahedral twist, has been used for the $N_2(NH)_2$ complexes, and a value of $e_\sigma/e_\pi = 10$ has been used for the N_2S_2 complexes, since the values (6.2–7.7) found for other N_2S_2 complexes[5f] increased with the tetrahedral twist.

Determination of kinetic parameters for the racemization process

Rate constants k for the racemization process (2) were obtained from the temperature-dependent proton spectra of exchanging diastereotopic protons using equations (5)[21a] and (6)[21b] and the

$$T \leqslant T_c\text{: } k(T) = 0.5\pi[2(\Delta\nu^{\circ 2} - \Delta\nu^2)]^{\frac{1}{2}} \quad (5)$$

$$T \geqslant T_c\text{: } k(T) = 0.5\pi\Delta\nu^\circ[(\Delta\nu^\circ/\nu_{\frac{1}{2}})^2 - (\nu_{\frac{1}{2}}/\Delta\nu^\circ)^2 + 2]^{\frac{1}{2}} \quad (6)$$

method used for other paramagnetic nickel(II) complexes[2c] with appropriate modifications for spin-equilibrium systems.[4b] Here T_c is the coalescence temperature for the resonances of exchanging protons, $\Delta\nu^\circ$ the chemical shift difference between the indicator protons in the absence of exchange and $\nu_{\frac{1}{2}}$ and $\Delta\nu$ are the observed linewidth of and chemical shift difference between the indicator protons, respectively. The diastereotopic indicator groups used are Me^4 (**1**–**7**), o^3 and m^3 (**8** and **9**), a and b (**1***–**6***) and Me^3 (**7*** and **8***). Values of $\Delta H^\ddagger$ and $\Delta S^\ddagger$ were derived from plots of $\ln(k/T)$ *vs.* $1/T$ using the Eyring equation (7).

$$k(T) = T(k_B/h)\exp(\Delta S^\ddagger/R)\exp[-\Delta H^\ddagger/(RT)] \quad (7)$$

Crystallography

The crystallographic experiments were performed at Aarhus University complex (**1**) and at Odense University (**3***). Details are given in Table 9. Data were collected at room temperature

‡‡ A molecular g value of 2.002 (the spin-only value) has been used in the conversion of equation (4) from the form in ref. 9 to the presented form;[2c] $g = \mu/[S(S + 1)]^{\frac{1}{2}}$ is probably larger in most cases, $\mu = 3.30\ \mu_B$ yields $g = 2.33$. However, use of the more correct g value has no significant effect on the thermodynamic parameters, *e.g.* $\Delta H = 17.0$ kJ mol^{-1} and $\Delta S = 39.6$ J K^{-1} mol^{-1} are calculated for complex **1*** in CD_2Cl_2 using $g = 2.33$ [found $\Delta H = 17.0 \pm 0.4$ kJ mol^{-1}, $\Delta S = 40.8 \pm 1.5$ J K^{-1} mol^{-1}, see Table 5(*b*)].

§§ Recent investigations[19a] have shown that the use of equation (4) may be problematic: in particular, the contact shift was found to be non-isotropic and the dipolar coupling to be of considerable importance for pseudo-tetrahedral Ni^{II}. However, as consistent results are obtained for the thermodynamic parameters derived by three different methods in the work described in ref. 1(*c*), one of which involves the use of the paramagnetic shifts and equation (4), we consider the present method still to be acceptable.

¶¶ Plots of chemical shifts *vs.* N_{hs}/T for protons H_i other than the indicator proton H_{ind} have been used as a control; straight lines with correlations close to unity and numerical values of $B_i < 10$ ppm[19b] for strongly coupled protons confirm reasonable estimates for A_{ind} and B_{ind} in the first step of the procedure.

Table 9 Crystal data and details of data collection and structure refinement for complexes **1** and **3***

	1	**3***
Formula	$C_{38}H_{38}N_8Ni$	$C_{16}H_{22}N_6NiS_2$
M	665.472	421.210
Crystal system	Triclinic	Monoclinic
Space group	*P*$\bar{1}$	*Cc*
a/Å	17.485(4)	9.121(3)
b/Å	11.298(3)	18.110(4)
c/Å	9.399(4)	11.531(1)
α/°	67.26(2)	—
β/°	82.84(2)	98.78(2)
γ/°	84.15(1)	—
U/Å^3	1696(1)	1882.4(8)
Crystal size/mm	0.80 × 0.30 × 0.25	0.36 × 0.43 × 0.16
Developed forms	Fracture	{100}{010}{001}
D_c/g cm^{-3}	1.303	1.486
Z	2	4
μ/cm^{-1}	6.11	12.12
Transmission factors	0.89–0.96	0.657–0.824
θ Limits/°	1–25	2–30
Octants collected	±*h*, −*k*, ±*l*	+ *h*, + *k*, ±*l*
Standard reflections	10 2 0, 0 4 −2	3 9 2
Fall-off in intensity (%)	3	4.8
No. unique data	5972	2340
No. observed data	4773	2144
[*n* in $I > n\sigma(I)$]	3.0	2.5
No. variables	577	227
R^a	0.037	0.079
R'^b	0.055	0.064
$\Delta\rho_{max}$, $\Delta\rho_{min}$/e Å^{-3}	0.24, −0.39	1.52(4),[c] −1.42(4)

[a] $R = \Sigma(|F_o| - |F_c|)/\Sigma|F_o|$. [b] $R' = [\Sigma w(|F_o| - |F_c|)^2/\Sigma w|F_o|^2]^{\frac{1}{2}}$, $w^{-1} = \{[\sigma_c(F^2) + 1.04F^2]^{\frac{1}{2}} - |F|\}^2$ (complex **1**), $\sigma^2(F)$ (**3***). [c] The highest residual peak is located 1.07 Å from Ni.

using Mo-Kα radiation (λ 0.710 73 Å). The least-squares refinements were based on *F* in both structures. The plotting program ORTEP II [22a] was used for the diagrams.

Complex 1. A dark red crystal grown from EtOH was used for the crystallographic experiment. The unit cell was refined using the setting angles from 24 reflections centred at positive and negative θ in the range 20–26°. A Huber diffractometer was used for this and for the intensity measurements. Two standard reflections were measured every 50. Step scans of 50 points were collected, integrated [22b] and the intensities corrected for Lorentz-polarization effects and for decay. Absorption corrections were done by Gaussian integration. The structure was solved by direct methods (SHELXS 86) [22c] and refined by full-matrix least-squares methods [22c] employing anisotropic thermal parameters for all non-hydrogen atoms. Hydrogen atoms were introduced at calculated positions confirmed by Fourier-difference maps.

Complex 3*. Dark green crystals were grown from MeCN–$CHCl_3$ (3:1). The cell constants were obtained by least-squares refinement from the setting angles of 25 reflections. Intensities were measured at room temperature using an Enraf-Nonius CAD-4F diffractometer. The intensity of a standard reflection was measured every 3 h and the decay corrected for. Data were corrected for Lorentz-polarization effects and for absorption.[22d] Relevant programs from XTAL 3.2 [22e] were used to solve (by an integrated Patterson and direct methods procedure) and to refine the structure (by block-diagonal least-squares refinement employing anisotropic thermal parameters for all non-hydrogen atoms). Hydrogen atoms were introduced at geometrically idealized positions [*d*(C–H) = 0.96 Å, *U*(H) = 0.06 Å^2].

Atomic coordinates, thermal parameters, and bond lengths and angles have been deposited at the Cambridge Crystallographic Data Centre (CCDC). See Instructions for Authors, *J. Chem. Soc., Dalton Trans.*, 1997, Issue 1. Any request to the CCDC for this material should quote the full literature citation and the reference number 186/491.

Acknowledgements

We gratefully acknowledge Professor O. P. Anderson, Colorado State University, for critical reading of the manuscript and for valuable comments, Mrs. B. Heinrich and Mrs. T. Meinel, Leipzig University, for technical assistance with collection of NMR spectra and Mrs. I. Pederson and Mr. O. T. Sørensen, Odense University (O.U.) for the mass spectra. Professor H. Toftlund, O.U., is acknowledged for providing laboratory facilities (A. la C.) and the Danish Natural Science Research Council and the Carlsberg Foundation for the diffractometers (R. H. and O. S.).

References

1 (*a*) L. H. Pignolet, W. DeW. Horrocks, jun., and R. H. Holm, *J. Am. Chem. Soc.*, 1970, **92**, 1855; (*b*) L. Que, jun. and L. H. Pignolet, *Inorg. Chem.*, 1973, **12**, 156; (*c*) H. Frydendahl, H. Toftlund, J. Becker, J. C. Dutton, K. S. Murray, L. F. Taylor, O. P. Anderson and E. R. T. Tiekink, *Inorg. Chem.*, 1995, **34**, 4467.
2 (*a*) R. Knorr, A. Weiss, H. Polzer and E. Räpple, *J. Am. Chem. Soc.*, 1977, **99**, 650; (*b*) L. E. Nivorozhkin, A. L. Nivorozhkin, M. S. Korobov, L. E. Konstantinovsky and V. I. Minkin, *Polyhedron*, 1985, **4**, 1701; (*c*) A. la Cour, B. Adhikhari, H. Toftlund and A. Hazell, *Inorg. Chim. Acta*, 1992, **202**, 145.
3 G. Hinsche, E. Uhlemann, D. Zeigan and G. Engelhardt, *Z. Chem.*, 1981, **21**, 414.
4 (*a*) A. L. Nivorozhkin, H. Toftlund, P. L. Jørgensen and L. E. Nivorozhkin, *J. Chem. Soc., Dalton Trans.*, 1996, 1215; (*b*) A. la Cour, M. Findeisen, A. Hazell, R. Hazell and G. Zdobinsky, *J. Chem. Soc., Dalton Trans.*, 1997, 121; (*c*) A. la Cour, M. Findeisen, R. Hazell, L. Hennig, C. E. Olsen and O. Simonsen, *J. Chem. Soc., Dalton Trans.*, 1996, 3437; (*d*) O. P. Anderson, A. la Cour, M. Findeisen, L. Hennig, O. Simonsen, L. F. Taylor and H. Toftlund, *J. Chem. Soc., Dalton Trans.*, 1997, 111; (*e*) L. Hennig, R. Kirmse, O. Hammerich, S. Larsen, H. Frydendahl, H. Toftlund and J. Becher, *Inorg. Chim. Acta*, 1995, **234**, 67.
5 (*a*) A. L. Nivorozhkin, H. Toftlund, L. E. Nivorozhkin, I. A. Kamenetskaya, A. S. Antsishkina and M. A. Porai-Koshits, *Transition Met. Chem.*, 1994, **19**, 319; (*b*) S. S. Sheldrick, R. Knorr and H. Polzer, *Acta Crystalogr., Sect. B*, 1979, **35**, 739; (*c*) D. Dale, *J. Chem. Soc. A*, 1967, 278; (*d*) N. A. Bailey and E. D. McKenzie, *Inorg. Chim. Acta*, 1980, **43**, 205; (*e*) N. A. Bailey, E. D. McKenzie and J. M. Worthington, *J. Chem. Soc., Dalton Trans.*, 1974, 1363; (*f*) B. Adhikhari, A. la Cour, R. Hazell, C. E. Olsen and H. Toftlund, unpublished work.
6 (*a*) A. D. Garnovskii, A. L. Nivorozhkin and V. I. Minkin, *Coord. Chem. Rev.*, 1993, **126**, 1; (*b*) A. L. Nivorozhkin, S. E. Konstantinovsky, L. E. Nivorozhkin, V. I. Minkin, T. G. Takhirov, O. A. Diachenko and D. B. Tagiev, *Izv. Akad. Nauk SSSR, Ser. Khim.*, 1990, 327 (in Russian).
7 S. K. Sur, *J. Magn. Reson.*, 1989, **82**, 169.
8 I. Y. Kvitko, L. V. Alam, N. I. Rtishchev, A. V. Eltsov, L. N. Kurovskaya and N. B. Chebotareva, *J. Gen. Chem. USSR* (*Engl. Transl.*), 1982, 2048.
9 R. H. Holm, *Acc. Chem. Res.*, 1969, **2**, 307.
10 H. Toftlund, A. L. Nivorozhkin, A. la Cour, B. Adhikhari, K. S. Murray, G. D. Fallon and L. E. Nivorozhkin, *Inorg. Chim. Acta*, 1995, **228**, 237.
11 A. L. Nivorozhkin, L. E. Nivorozhkin, V. I. Minkin, T. G. Takhirov and O. A. Diachenko, *Polyhedron*, 1991, **10**, 179.
12 R. H. Holm and K. Swaminathan, *Inorg. Chem.*, 1962, **1**, 599.
13 R. H. Holm, G. W. Everett, jun., and A. Chakravorty, *Prog. Inorg. Chem.*, 1966, **7**, 83.
14 (*a*) D. H. Gerlach and R. H. Holm, *J. Am. Chem. Soc.*, 1969, **91**, 3457; (*b*) I. Bertini, L. Sacconi and G. P. Speroni, *Inorg. Chem.*, 1972, **11**, 1323; (*c*) H. R. Engeseth, D. R. McMillin and E. L. Ulrich, *Inorg. Chim. Acta*, 1982, **67**, 145; (*d*) E. M. Martin and R. D. Bereman, *Inorg. Chim. Acta*, 1991, **188**, 233.
15 (*a*) D. A. Cruse and M. Gerloch, *J. Chem. Soc., Dalton Trans.*, 1976, 152; (*b*) R. H. Holm and K. Swaminathan, *Inorg. Chem.*, 1963, **2**, 181.
16 M. Gerloch, *Coord. Chem. Rev.*, 1990, **99**, 117.

17 (*a*) R. Knorr and A. Weiss, *Chem. Ber.*, 1981, **114**, 2104; (*b*) R. Knorr and F. Ruf, *J. Am. Chem. Soc.*, 1979, **101**, 5424; (*c*) R. Knorr and F. Ruf, *Angew. Chem.*, 1984, **96**, 350.
18 J. Becher, K. Pluta, N. Krake, K. Brøndum, N. J. Christensen and M. V. Vinader, *Synthesis*, 1985, 530; J. Becher, P. L. Jørgensen, H. Frydendahl and B. F. Hansen, *Synthesis*, 1991, 603.
19 (*a*) B. R. McGarvey, *Inorg. Chem.*, 1995, **34**, 6000; (*b*) W. D. Perry and R. S. Drago, *J. Am. Chem. Soc.*, 1971, **93**, 2183.
20 A. B. P. Lever, *Inorganic Electronic Spectroscopy*, 2nd edn., Elsevier, Amsterdam, 1984, pp. 818–820.
21 (*a*) H. S. Gutowsky and C. H. Holm, *J. Chem. Phys.*, 1956, **25**, 1228; (*b*) A. Allerhand, H. S. Gutowsky, J. Jonas and R. A. Meinzer, *J. Am. Chem. Soc.*, 1966, **88**, 3185.
22 (*a*) C. K. Johnson, ORTEP II, Report ORNL-5138, Oak Ridge National Laboratory, TN, 1976; (*b*) M. S. Lehmann and F. K. Larsen, *Acta Crystallogr., Sect. A*, 1974, **30**, 580; (*c*) G. M. Sheldrick, SHELXS 86, Program for the Solution of Crystal Structures, University of Göttingen, 1986; (*d*) R. Norrestam and K. Nielsen, Technical University of Denmark, personal communication, 1982; (*e*) S. R. Hall, H. D. Flack and J. M. Stewart (Editors), *XTAL 3.2 Reference Manual*, University of Western Australia and Maryland, 1992.

Received 23*rd December* 1996; *Paper* 6/08598I